Response of global soil consumption of atmospheric methane to changes in atmospheric climate and nitrogen deposition

Qianlai Zhuang,[1,2,3] Min Chen,[1] Kai Xu,[1] Jinyun Tang,[1] Eri Saikawa,[3] Yanyu Lu,[1] Jerry M. Melillo,[4] Ronald G. Prinn,[3] and A. David McGuire[5]

Received 14 July 2012; revised 12 May 2013; accepted 9 June 2013.

[1] Soil consumption of atmospheric methane plays an important secondary role in regulating the atmospheric CH_4 budget, next to the dominant loss mechanism involving reaction with the hydroxyl radical (OH). Here we used a process-based biogeochemistry model to quantify soil consumption during the 20th and 21st centuries. We estimated that global soils consumed 32–36 Tg CH_4 yr^{-1} during the 1990s. Natural ecosystems accounted for 84% of the total consumption, and agricultural ecosystems only consumed 5 Tg CH_4 yr^{-1} in our estimations. During the twentieth century, the consumption rates increased at 0.03–0.20 Tg CH_4 yr^{-2} with seasonal amplitudes increasing from 1.44 to 3.13 Tg CH_4 $month^{-1}$. Deserts, shrublands, and xeric woodlands were the largest sinks. Atmospheric CH_4 concentrations and soil moisture exerted significant effects on the soil consumption while nitrogen deposition had a moderate effect. During the 21st century, the consumption is predicted to increase at 0.05-1.0 Tg CH_4 yr^{-2}, and total consumption will reach 45–140 Tg CH_4 yr^{-1} at the end of the 2090s, varying under different future climate scenarios. Dry areas will persist as sinks, boreal ecosystems will become stronger sinks, mainly due to increasing soil temperatures. Nitrogen deposition will modestly reduce the future sink strength at the global scale. When we incorporated the estimated global soil consumption into our chemical transport model simulations, we found that nitrogen deposition suppressed the total methane sink by 26 Tg during the period 1998–2004, resulting in 6.6 ppb higher atmospheric CH_4 mixing ratios compared to without considering nitrogen deposition effects. On average, a cumulative increase of every 1 Tg soil CH_4 consumption decreased atmospheric CH_4 mixing ratios by 0.26 ppb during the period 1998–2004.

Citation: Zhuang, Q., M. Chen, K. Xu, J. Tang, E. Saikawa, Y. Lu, J. M. Melillo, R. G. Prinn, and A. D. McGuire (2013), Response of global soil consumption of atmospheric methane to changes in atmospheric climate and nitrogen deposition, *Global Biogeochem. Cycles*, *27*, doi:10.1002/gbc.20057.

1. Introduction

[2] Methane (CH_4), a potent greenhouse gas and a reactive chemical compound in the atmosphere, affects the global climate system and atmospheric chemistry. It is 25 times more effective, on a per-unit-mass basis, than carbon dioxide (CO_2) in absorbing long-wave radiation on a 100 year time horizon [*Forster et al*., 2007]. It contributes 0.48 W m^{-2} to the total anthropogenic radiative forcing of 2.43 W m^{-2} by well-mixed greenhouse gases [*Forster et al*., 2007] and has an indirect effect of 0.13 W m^{-2} through the formation of other greenhouse gases, mainly tropospheric ozone and stratospheric water vapor [*Lelieveld et al*., 1998]. Its atmospheric concentrations have increased about 1.5 times since 1750 to the year 2005 level of 1774.62 ± 1.22 ppb observed by U.S. National Oceanic and Atmospheric Administration (NOAA)/Global Monitoring Division [*Dlugokencky et al*., 2005] and 1774.03 ± 1.68 ppb observed by the Advanced Global Atmospheric Gases Experiment (AGAGE) network with a greater interannual variability in recent decades [*Forster et al*., 2007]. More recent observation estimates that the global mean atmospheric CH_4 concentrations in 2009 reached 1794 ppb [*Dlugokencky et al*., 2009]. The significant interannual variations of atmospheric CH_4 concentrations include (1) abruptly declining in 1992; (2) rising in 1993 and 1994 and peaking in 1998 [*Dlugokencky et al*., 1996; *Cunnold et al*., 2003]; (3) approaching a steady state during 1999 and 2002 [*Dlugokencky et al*., 2003]; (4) reaching an apparent steady state from 1999 to 2005/2006 [*Dlugokencky et al*., 2009]; and (5) rising again since 2006,

[1]Department of Earth, Atmospheric, and Planetary Sciences, Purdue University, West Lafayette, Indiana, USA.
[2]Department of Agronomy, Purdue University, West Lafayette, Indiana, USA.
[3]Department of Earth, Atmospheric, and Planetary Sciences, Massachusetts Institute of Technology, Cambridge, Massachusetts, USA.
[4]Ecosystems Center, Marine Biological Laboratory, Woods Hole, Massachusetts, USA.
[5]Department of Biology and Wildlife, University of Alaska Fairbanks, Fairbanks, Alaska, USA.

Corresponding author: Q. Zhuang, Department of Earth, Atmospheric, and Planetary Sciences, Purdue University, 550 Stadium Mall Dr., West Lafayette, IN 47907-2051, USA. (qzhuang@purdue.edu)

0886-6236/13/10.1002/gbc.20057

specifically the increases are 8.3 ± 0.6 and 4.4 ± 0.6 ppb during 2007 and 2008, respectively [*Rigby et al*., 2008; *Dlugokencky et al*., 2009]. To date, these dynamics have not been well understood as to their sources and sinks [e.g., *Zhuang et al*., 2009; *Prinn et al*., 2005; *Curry*, 2007].

[3] Biogeochemistry models have been extensively used to quantify the regional and global land surface emissions, or sources, of atmospheric CH_4 [e.g., *Walter et al*., 2001; *Cao et al*., 1995; *Potter et al*., 1996; *Zhuang et al*., 2004]. The global chemical transport models in combination with satellite and in situ observational data have also been used to constrain surface emissions [e.g., *Hein et al*., 1997; *Houweling et al*., 1999; *Bergamaschi et al*., 2005, 2009; *Mikaloff Fletcher et al*., 2004; *Dentener et al*., 2003; *Butler et al*., 2004; *Bousquet et al*., 2006; *Chen and Prinn*, 2006; *Frankenberg et al*., 2008; *Rigby et al*., 2008]. Based on these studies, it has been estimated that the current emissions from the Earth's surface range from 503 to 610 Tg CH_4 yr^{-1} [*Forster et al*., 2007]. A more recent synthesis study identified the challenges to more accurately quantifying biogenic emissions from major source regions and sectors on the Earth's surface, including the Amazon, rice paddies, and the Arctic [*Zhuang et al*., 2009].

[4] In terms of CH_4 sinks, the atmospheric hydroxyl radicals (OH) are found to be a major sink based on model and observational studies of methyl chloroform [e.g., *Prinn et al*., 2001, 2005; *Krol and Lelieveld*, 2003; *Bousquet et al*., 2005; *Montzka et al*., 2011]. After the OH sink, soil uptake due to methanotrophy is the second largest sink at 15–45 Tg CH_4 yr^{-1} [*Forster et al*., 2007]. Since soil consumption rates are of a similar magnitude to the rate of CH_4 accumulation in the atmosphere, any significant changes in this sink will affect the net accumulation of this potent greenhouse gas in the atmosphere [*Dutaur and Verchot*, 2007]. To date, the amount of global soil consumption has been quantified with numerous biogeochemistry models [e.g., *Potter et al*., 1996; *Ridgwell et al*., 1999; *Curry*, 2007, 2009; *Spahni et al*., 2011; *Melton et al*. 2012]. These studies consider the effects of changes in atmospheric CH_4 concentrations, land use, and climate. However, nitrogen deposition has not been included in these analyses, despite it having been shown to significantly affect the consumption rate [e.g., *King*, 1997; *Zhang et al*., 2008; *Menyailo et al*., 2008].

[5] Here we used an extant biogeochemistry model, the Terrestrial Ecosystem Model (TEM) [*Melillo et al*., 1993; *Zhuang et al*., 2004, 2006, 2007], to provide a more comprehensive quantification of global soil consumption in both natural and agricultural ecosystems in a spatially and temporally explicit manner for the 20th and 21st centuries. In this analysis, we explicitly evaluated the nitrogen deposition effects in addition to multiple stresses including the changes of climate, atmospheric CH_4 concentrations, and land use at the global scale. Using the global soil consumption rates calculated from TEM, we also ran a three-dimensional global chemical transport model, the Model for Ozone and Related Tracers version 4 (MOZART v4) [*Emmons et al*., 2010] to evaluate the role of this sink in affecting atmospheric mixing ratios for recent years.

2. Method

2.1. Overview

[6] We first revised an earlier version of the TEM by incorporating the effects of changes in nitrogen deposition, soil moisture, and atmospheric CH_4 concentrations on methanotrophy rates and also CH_4 transport between soils and the atmosphere. Second, we used field data for CH_4 consumption rates of various ecosystems (ranging from tundra to tropical forests to cropland ecosystems) to parameterize the model. Spatially explicit data for climate, soils, atmospheric nitrogen deposition, land use and land cover change, as well as atmospheric CH_4 concentrations, are then used to extrapolate the parameterizations and overall model to global terrestrial ecosystems at a 0.5° by 0.5° (latitude by longitude) spatial resolution over the 20th and 21st centuries. A set of simulations was conducted to examine the various effects on global soil consumption. Third, we conducted a set of simulations using MOZART v4 to examine how different degrees of global soil methane uptake affect atmospheric methane mole fractions between 1998 and 2004.

2.2. Model Modification

[7] The Terrestrial Ecosystem Model is a process-based biogeochemistry model that couples carbon, nitrogen, water, and heat processes in terrestrial ecosystems to simulate ecosystem carbon and nitrogen dynamics (TEM) [*Melillo et al*., 1993; *Zhuang et al*., 2003, 2004, 2007]. In TEM, methanogenesis (CH_4 production) and methanotrophy (CH_4 consumption) are affected by hydrological and soil thermal dynamics, in addition to other biological and chemical controls, in both non-permafrost and permafrost ecosystems [*Zhuang et al*., 2001, 2002, 2004]. Specifically, methanotrophy is modeled as an aerobic process that occurs in the unsaturated zone of the soil profile.

[8] The hourly methanotrophy rates within each 1 cm layer of the soil profile are modeled as a function of soil CH_4 concentrations, soil temperature, soil moisture, and redox potentials [*Zhuang et al*., 2004]. In this study, we modified the algorithm for methanotrophy by incorporating the effects of water inhibition on atmospheric CH_4 diffusivity to soils and the effects of nitrogen deposition and changes in atmospheric CH_4 concentrations on the methanotrophy rate, $M_o(z,t)$, at soil depth z and time t as

$$M_O(z,t) = O_{\mathrm{MAX}} \times f(C_M(z,t)) \times f(T_{\mathrm{SOIL}}(z,t)) \cdot f(E_M(z,t)) \times f(R_{\mathrm{OX}}(z,t)) \times f\left(N_{dp}(z,t)\right) \cdot f(D_{ms}(z,t)) \quad (1)$$

where O_{MAX} is the ecosystem-specific maximum oxidation rate that typically ranges between 0.3 and 360 μmol L^{-1} h^{-1} [*Segers*, 1998]; $f(C_M(z,t))$ is a multiplier that enhances methanotrophy rate with increasing soil CH_4 concentrations using a Michaelis-Menten function with a half-saturation constant (K_{CH4}) that varies across ecosystems; $f(T_{\mathrm{SOIL}}(z,t))$ is a multiplier that enhances methanotrophy rates with increasing soil temperatures using a Q_{10} function with Q_{10} coefficients (O_{Q10}) and reference temperatures (T_{OR}) that vary across ecosystems; $f(E_{\mathrm{SM}}(z,t))$ is a multiplier to account for the biological limiting effect that diminishes methanotrophy rates if the soil moisture is not at an optimum level ($M_{v\mathrm{opt}}$); and $f(R_{\mathrm{OX}}(z,t))$ is a multiplier that enhances methanotrophy rates as redox potentials increase linearly from −200 mV to 200 mV (as redox potentials become greater than 200 mV, $f(R_{\mathrm{OX}}(z,t))$ is set equal to 1.0) [*Zhang et al*., 2002].

[9] Methanotrophy is also assumed to cease if soil moisture reaches a critical minimum ($M_{v\mathrm{min}}$) or maximum

Table 1. Parameterization Sites of Natural and Managed Ecosystems in This Study[a]

Site Name	Location (Longitude/Latitude)	Elevation (m)	Vegetation	Driving Climate Data	Observed Data	Sources and Comments
Puerto Rico (PR)	65°45′W/18°19′N	103	Tropical forest	NCEP[a] 1948–2005	CH_4 flux of April 1984	*Keller et al.* [1986]
Nunn, Colorado (NC)	104°45′W/40°48′N	1584	Grassland	NOAA[b] 1981–1996	CH_4 flux of 1990	*Mosier et al.* [1991]
Petersham, Massachusetts (BFT)	72°10′W/42°30′N	277	Temperate coniferous forests	NOAA 1982–1989	CH_4 flux of May–December 1988	*Castro et al.* [1995]
Petersham, Massachusetts (BFD)	72°10′W/42°30′N	277	Temperate deciduous forests	NOAA 1982–1989	CH_4 flux of May–December 1988	*Castro et al.* [1995]
Heidelberg,Germany (HGX)	8°36′E/49.4°N	217	Xeric woodlands	NCEP 1948–2005	Annual consumption of 1987–1988	*Born et al.* [1990]
Heidelberg,Germany (HGM)	8°36′E/49.4°N	217	Mediterranean shrublands	NCEP 1948–2005	Annual consumption of 1987–1988	*Born et al.* [1990]
Petersham, Massachusetts (BFE)	72°10′W/42°30′N	277	Temperate evergreen broadleaf	NOAA 1982–1989	CH_4 flux of May–December 1988	*Castro et al.* [1995]
Shoshone Mountain, Nevada (MD)	116°2′/36°37′N	2477	Desert	NOAA 1985–1994	CH_4 flux of January 1989–June 1991	*Striegl et al.* [1992]
Barro Colorado Island, Las Pavas, Panama (BCI)	9°10′N/79°50′W	149	C3 rice	CRU2[c] 1988	Daily soil CH_4 consumption 1988	*Keller et al.* [1990]
Ingham, north Queensland (INQ)	18°42′S/146°12′E	108	C4 sugarcane	CRU2 1996	Daily CH_4 consumption of 1996	*Weier* [1999]
Varanasi, Gangetic Plains, India (VA)	25°18′N/80°1′W	27	C3 rice	CRU2 1995	Seasonal CH_4 consumption of 1995	*Singh et al.* [1999]
Roadside Farm, Iowa (IW)	41°56′17″N/93°23′23″W	329	C4 corn-soybean	NOAA 1993	Seasonal CH_4 fluxes of 1993	*Chan and Parkin* [2001]
Gullane, Edinburgh, UK (GUK)	56°27.3′N/2°49′50.2″W	234	C3 wheat	CRU2 1994–1995	Daily CH_4 consumption of 1994–1995	*Dobbie and Smith* [1996]
Munich, Germany (MG)	48°8′20.86″N/11°34′ 48.7″E	494	C4 sunflower	CRU2 1992–1993	Hourly CH_4 consumption of 1992–1993	*Flessa et al.* [1995]

[a]NCEP: National Centers for Environmental Prediction.
[b]NOAA: National Oceanic and Atmospheric Administration.
[c]CRU2: Climatic Research Unit version 2.0.

($M_{v\max}$) value. These critical soil moisture values, along with the optimum soil moisture ($M_{v\text{opt}}$), are assumed to vary among ecosystems [see *Zhuang et al.*, 2004, equation (B3)]. The term $f(N_{dp}(z,t))$ represents the effects of nitrogen deposition on the soil CH_4 consumption rate, and the term $f(D_{ms}(z,t))$ represents the moisture limiting effect on CH_4 consumption through its effects on atmospheric CH_4 diffusivity to soils. In comparison to our original formulation of methanotrophy, terms $f(N_{dp}(z,t))$ and $f(D_{ms}(z,t))$ are new [*Zhuang et al.*, 2004]. To account for the inhibitive effects of nitrogen deposition (mainly NH_x including NH_3 and NH_4) on soil CH_4 consumption, we first modeled the distribution of C_{NHx} in soil profiles (μmol gdw^{-1}; μmol per gram dry weight) at depth z (cm):

$$C_{NHx}(z) = \text{Dep}_{NHx}/14.0 \times A \times \exp(-A \times z)/(D_{\text{bulk}} \times 10) \quad (2)$$

[10] Here Dep_{NHx} (mg m^{-2}) is the total NH_x deposition in a certain month, with the assumption that the depth interval is 1 cm. Coefficient A (dimensionless) was estimated to be 0.227 based on *Schnell and King* [1994]. The soil bulk density, D_{bulk} (g cm^{-3}) is calculated based on soil texture [*Saxton et al.*, 1986]:

$$D_{\text{bulk}} = 2.65 \times \left[0.668 + 7.251 \times 10^{-4} \times \text{sand}\% - 0.1276 \cdot \log_{10}(\text{clay}\%)\right] \quad (3)$$

[11] At a given level of CH_4 concentrations at depth z (cm), the inhibition rate is calculated as

$$f\left(N_{dp}(z,t)\right) = \begin{cases} 0.2306 \times \text{InhibMax}(z) \times \left[\begin{array}{l} \log_{10}(CH_4(\text{ppm})) \\ -\log_{10}CH_{4_{\min}} \end{array}\right] \\ 0; \text{otherwise} \end{cases}$$
$$\cdot[\log_{10}CH_{4_{\max}} - \log_{10}(CH_4(\text{ppm}))]; \quad (4)$$
$$\text{if } \log_{10}CH_{4_{\min}} < \log_{10}(CH_4(\text{ppm})) < \log_{10}CH_{4_{\max}}$$

[12] Here $\log_{10}CH_{4_{\min}} = -0.2434$ and $\log_{10}CH_{4_{\max}} = 3.9332$ based on Figure 7 in *Schnell and King* [1994]. The maximum inhibition rate at depth z (cm) at a given level of NH_x concentrations at depth z (InhibMax (z)) was then calculated as

$$\text{InhibMax}(z) = C_{NH_x}(z) \times d\text{Inhib} \quad (5)$$

where dInhib is the maximum rate of inhibition for 1 μmol gdw^{-1} NH_x, which is estimated as 60% based on *Schnell and King* [1994].

[13] The moisture limiting effect on CH_4 consumption $f(D_{ms}(z,t))$ is modeled via affecting atmospheric CH_4 diffusivity:

$$f(D_{ms}(z,t)) = -\left(\frac{\text{SM} - \text{SM}_{\min}}{\text{SM}_{\text{sat}} - \text{SM}_{\min}}\right)^{\gamma} + 1 \quad (6)$$

[14] Here at the minimum soil moisture $\text{SM}_{\min}$, $f(D_{ms}(z,t))$ is equal to 1.0. As SM approaches the saturation point SM_{sat}, the diffusivity $D(z)$ decreases as $f(D_{ms}(z,t))$ decreases. We set a minimum value of 0.0001 for $f(D_{ms}(z,t))$ since in saturated soils, the diffusivity is usually on the order of 4 times smaller than in dry soils [*Walter* and *Heimann*, 2000]. In equation (6), γ, a parameter depending on the aggregation structure, is set at 1.0.

Table 2. Model Parameters for Various Natural and Agricultural Ecosystems[a]

Site	O_{MAX}	K_{CH4}	O_{Q10}	T_{OR}
PR	1.0	15.0	1.2	5.0
NC	1.0	15.0	2.0	3.0
BFT	2.0	15.0	5.5	2.5
BFD	2.0	15.0	4.4	2.0
HGX	1.0	10.0	5.0	1.9
HGM	1.0	10.0	5.0	1.9
BFE	2.0	15.0	4.4	2.0
MD	1.0	10.0	1.1	1.9
BCI[b]	1.0	15.0	0.8	3.0
INQ[b]	1.0	10.0	2.9	5.0
VA[b]	1.0	15.0	2.5	4.5
IW[b]	1.0	10.0	0.8	5.0
GUK[b]	2.0	15.0	1.8	5.0
MG[b]	1.0	10.0	0.3	2.0

[a] O_{MAX} is a maximum methane oxidation rate (μmol L^{-1} h^{-1}). K_{CH4} is a Michaelis-Menten coefficient to account for atmospheric methane concentration effects (μmol L^{-1}). O_{Q10} is an ecosystem-specific Q_{10} coefficient to account for soil temperature effects on methanotrophy. T_{OR} is the reference soil temperature to account for soil temperature effects on methanotrophy (°C). Site names are in Table 1.
[b] Agricultural sites.

[15] To compute the CH_4 consumption in soils, we solved the steady state transport equation for the soil profile at a 1 cm depth step:

$$\frac{\partial}{\partial z}\left(D(z)\frac{\partial C_{CH_4}}{\partial z}\right) - M_O(z) = 0 \tag{7}$$

using the following boundary conditions:

$$\begin{cases} C_{CH_4}(0) = C_{CH_4atm}, & \text{at } z = 0 \\ \dfrac{d}{dz}C_{CH_4} = 0, & \text{at } z = z_b \end{cases} \tag{8}$$

[16] The diffusion coefficient $D(z)$ (with units of cm^{-2} h^{-1}) is modeled as a function of soil texture. Equation (7) is solved for CH_4 concentrations at different depths from the soil surface to a prescribed bottom level z_b [see *Zhuang et al.*, 2004]. The updated CH_4 concentrations are used to model $f(C_M(z,t))$ in equation (1). Total CH_4 consumed in the soil column (F_{cons}) within an hour is calculated based on the following:

$$F_{cons} = \int_0^{Z_b} M_O(z)dz \tag{9}$$

[17] Here Z_b is the lower boundary of the soil depth (cm), which is set to 100 cm.

2.3. Model Parameterization and Extrapolation

[18] We parameterized TEM for representative ecosystem types of both natural and agricultural ecosystems. The information on climate, soils, and observed consumption flux data for the calibration sites is documented in Table 1. The calibration was done by running TEM for the observational period driven with the corresponding local meteorological or climatic data at each site. The climate data from Climatic Research Unit (CRU) [*Mitchell and Jones*, 2005] or re-analysis data from the National Centers for Environmental Prediction (NCEP; http://www.ncep.noaa.gov/) are used (Table 1). Agricultural ecosystems were parameterized for both C3 and C4 crops (Table 2). Parameters in Table 2 were adjusted to allow the simulated daily average CH_4 consumption rates to match the observed daily average data with a tolerance of 1%. Specifically, based on the prior knowledge about the values of these four parameters for each site, we used a trial-and-error method to alter their values in model simulations while other parameters of TEM were kept as is. Comparison between the simulated and observed average daily consumption rates for the observation period was conducted to see if the tolerance was reached for each simulation. We iterated these steps until the tolerance value was met to determine the parameter values (Table 2). These site-level parameters were extrapolated to each 0.5° × 0.5° (latitude × longitude) pixel of the global natural ecosystem map that consists of 11 plant functional types (Table 3). For agricultural ecosystem pixels, C3 and C4 parameterizations were extrapolated with an assumption that the land area was occupied equally with these two types of crops. BCI and INQ parameterizations were used for C3 and C4 crop ecosystems for the pixels in the Southern Hemisphere. Site parameterizations of BCI and IW were used for C3 and C4 crop ecosystems, respectively, in the region between 0°N and 45°N. Sites GUK and MG parameterizations were used for the pixels with C3 and C4 crop ecosystems, respectively, above 45°N.

2.4. Spatially Explicit Data Organization for Global Simulations

[19] To make spatially and temporally explicit estimates of CH_4 consumption at the global scale with TEM, we utilized the data of land cover, soils, climate, and leaf area index (LAI) from a variety of sources at a spatial resolution of 0.5° latitude × 0.5° longitude. The land cover data include potential vegetation distribution [*Melillo et al.*, 1993], soil texture [*Zhuang et al.*, 2003], and water pH in soils [*Carter and Scholes*, 2000].

[20] Similar to earlier versions of TEM, the vegetation and soil texture data sets were used to assign vegetation- and

Table 3. Regional Soil Methane Consumption (Tg CH_4 yr^{-1}) for Both Natural (NE) and Agricultural Ecosystems (AE) in the 1990s, Partitioned to Different Latitude Bands[a]

	45°S South		0°S–45°S		0°N–45°N		45°N North		Global	
	NE	AE	NE	AE	NE	AE	NE	AE	NE	AE
S1	0.16	/	9.62	/	21.33	/	4.63	/	35.75	/
S2	0.16	/	9.68	/	21.18	/	4.56	/	35.58	/
S3	0.16	/	9.14	/	18.69	/	4.33	/	32.33	/
S4	0.15	0.01	7.79	1.21	14.64	3.37	4.04	0.54	26.62	5.13

[a] S3 and S4 simulations are with 2 year NH_x lag effects on consumption.

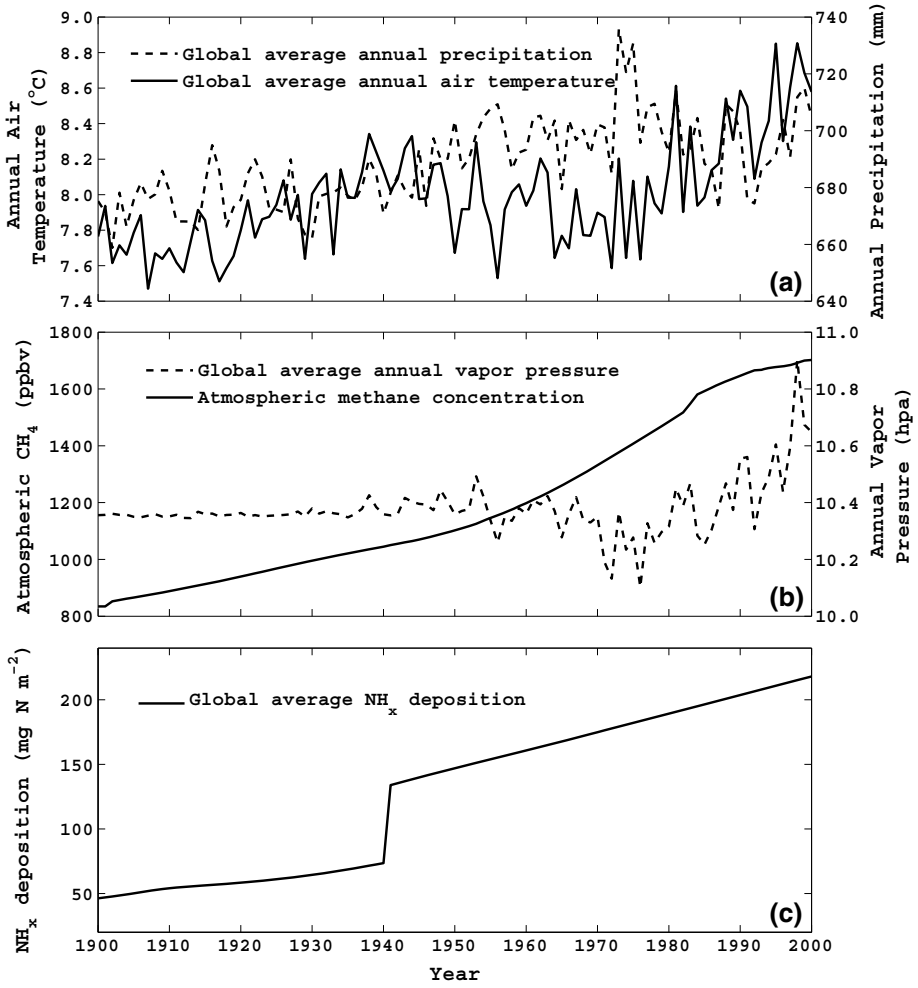

Figure 1. Historical climate, atmospheric CH_4 concentrations, and atmospheric NH_x deposition from 1900 to 2000 are based on *Mitchell and Jones* [2005], *Etheridge et al*. [1998], *Globalview-CH4* [2005], and *Galloway et al*. [2003], respectively.

texture-specific parameters to each grid cell. Agricultural grid cells in tropical, temperate, and northern high-latitude regions were assigned with different parameterizations for C3 and C4 crops, respectively (Table 2). The remaining spatially explicit data sets needed to provide inputs into the calculation of CH_4 consumption included those for wet soils and the fractional inundation of wetlands to derive the proportion of uplands within each 0.5° × 0.5° grid cell [*Matthews* and *Fung*, 1987]. Daily climate data sets were developed from the historical monthly air temperature,

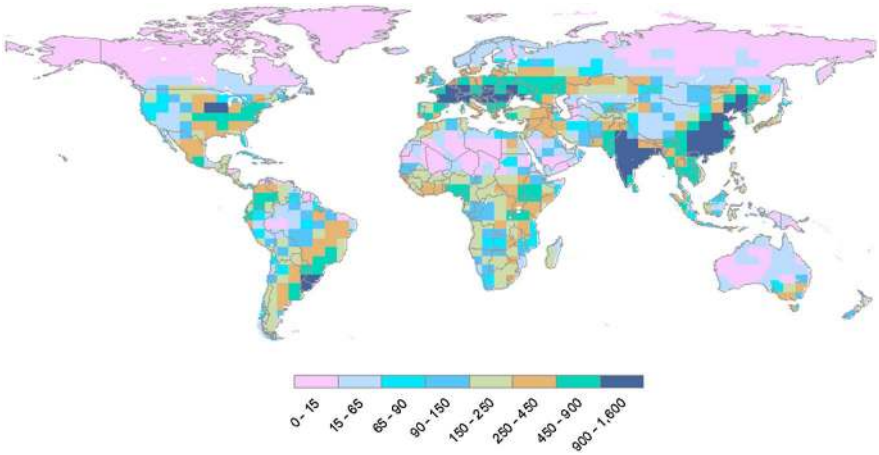

Figure 2. Global atmospheric NH_x deposition in the 1990s (mg N m^{-2} yr^{-1}) based on *Galloway et al*. [2003].

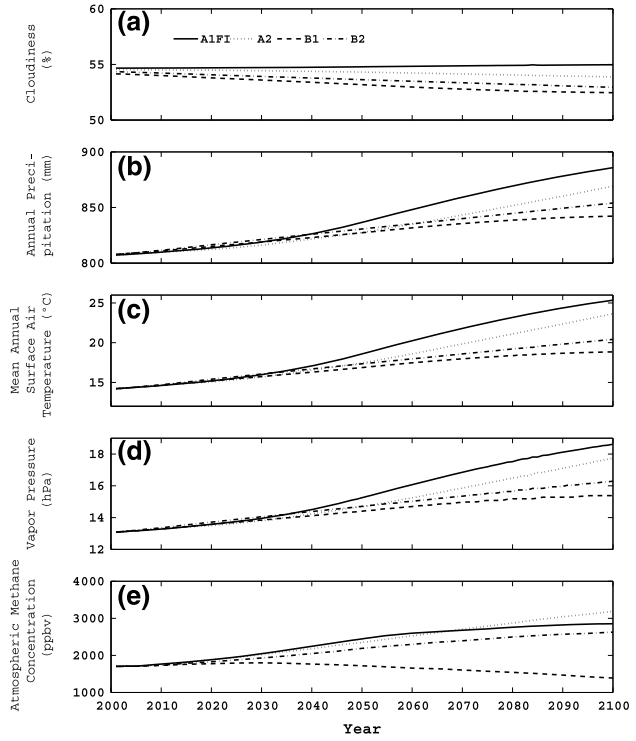

Figure 3. Climate and atmospheric CH_4 concentrations during the 21st century [*Forster et al*., 2007]: (a) cloudiness (%), (b) annual precipitation (mm), (c) mean annual surface air temperature (°C), (d) vapor pressure (hPa), and (e) atmospheric methane concentrations (ppb).

precipitation, vapor pressure, and cloudiness data sets [*Mitchell and Jones*, 2005] of the Climatic Research Unit (CRU) of the University of East Anglia in the United Kingdom (Figure 1a). Monthly LAI data required to simulate soil moisture in TEM are from *Zhuang et al*. [2004]. We used the data of 1992 for each year of the period 1993–2000 based on the data of *McGuire et al*. [2001] to extend the land cover and land use data to cover the twentieth century.

[21] We used the data of atmospheric CH_4 mixing ratio [units: parts per billion (ppb)] from *Etheridge et al*. [1998] (ice cores) and *Globalview-CH4* [2005] to develop the transient atmospheric CH_4 concentration data with units of μM (10^{-3} mol m^{-3}):

$$(CH_4)_{uM} = \frac{p}{R \times T}(CH_4)_{ppb} \times 10^{-6} \quad (10)$$

where p is atmospheric pressure (Pa), R is the universal gas constant (8.314472 J mol^{-1} K^{-1}), and T is air temperature (K). We used the mean annual surface air temperature data from *Smith and Reynolds* [2005], the observed atmospheric CH_4 concentration ($(CH4)_{ppb}$) record, and the standard atmospheric pressure for the calculation (Figure 1b).

[22] A spatially explicit data set of NH_x deposition from 1900 to 2000 is developed at a 0.5° spatial resolution (Figure 1c). The spatial variation of the magnitudes of NH_x deposition was based on the data for the years 1860 and 1993 (see http://daac.ornl.gov/CLIMATE/guides/global_N_deposition_maps.html). The original NH_x data have units of mg N m^{-2} yr^{-1} at a spatial resolution of 5° (longitude) by 3.75° (latitude). Here we scaled these NH_x deposition data with information from Figure 1a in *Galloway et al*. [2003] for the period from 1860 to 1940. From 1941 to 2000, the NH_x deposition rates were estimated based on these NH_x data and population information (see http://www.theworldeconomy.org/publications/worldeconomy/statistics.htm). The jump of NH_x deposition may be due to the industrial development, population rising, and agricultural fertilizer increases since 1940 (Figure 1c). The linear relationship between NH_x deposition and population was assumed based on the fact that most of the reactive nitrogen was created for agricultural production of food to support the population [*Galloway et al*., 2003]. Spatial heterogeneity of NH_x distribution was considered in developing these spatial data by grouping the population into 13 different subregions including Western Europe, Eastern Europe, Former USSR, United States of America, other Western offshoots, Mexico, other Latin America, Japan, China, India, other Asia, Africa, and Australia (its population from 1901 onward information is obtained from Australian Bureau of Statistics). Specifically, for the period from 1860 to 1940, scaling factors were derived by assuming that (1) the spatial pattern of NH_x deposition was constant and (2) the ratio of the overall NH_x deposition in a given year to that in 1860 is equal to the ratio of the total reactive nitrogen creation in the given year to that in 1860 (where the latter is described in Figure 1a in *Galloway et al*. [2003]). For the period from 1941 to 2000, a scaling factor, defined as the ratio of the NHx deposition in a given year to that in 1993, was assumed to be (1) as constant in any of the 13 subregions for the given year and (2) equal to the ratio of the human population in that year to

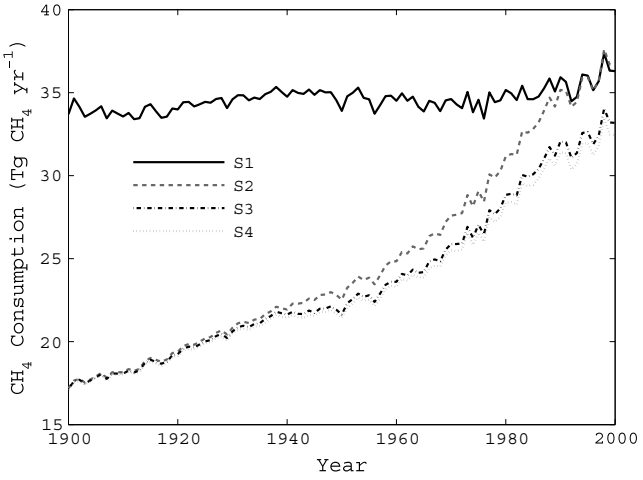

Figure 4. Annual global soil methane consumption (Tg CH_4 yr^{-1}) from 1900 to 2000: The estimates are derived from the simulations driven with changes of climate, atmospheric CH_4 concentrations, atmospheric NH_x deposition, and land use change. The effects of atmospheric NH_x deposition are assumed to be effective within a 2 year time horizon. Simulation S1 is driven with fixed atmospheric CH_4 concentration at 0.075 μM, but with transient climate throughout the century. Simulation S2 is driven with transient climate and atmospheric CH_4 concentrations. Simulation S3 is driven with transient climate, atmospheric CH_4 concentrations, and NH_x deposition. Simulation S4 is driven with transient data of climate, CH_4 concentrations, NH_x deposition, and land use and land cover change.

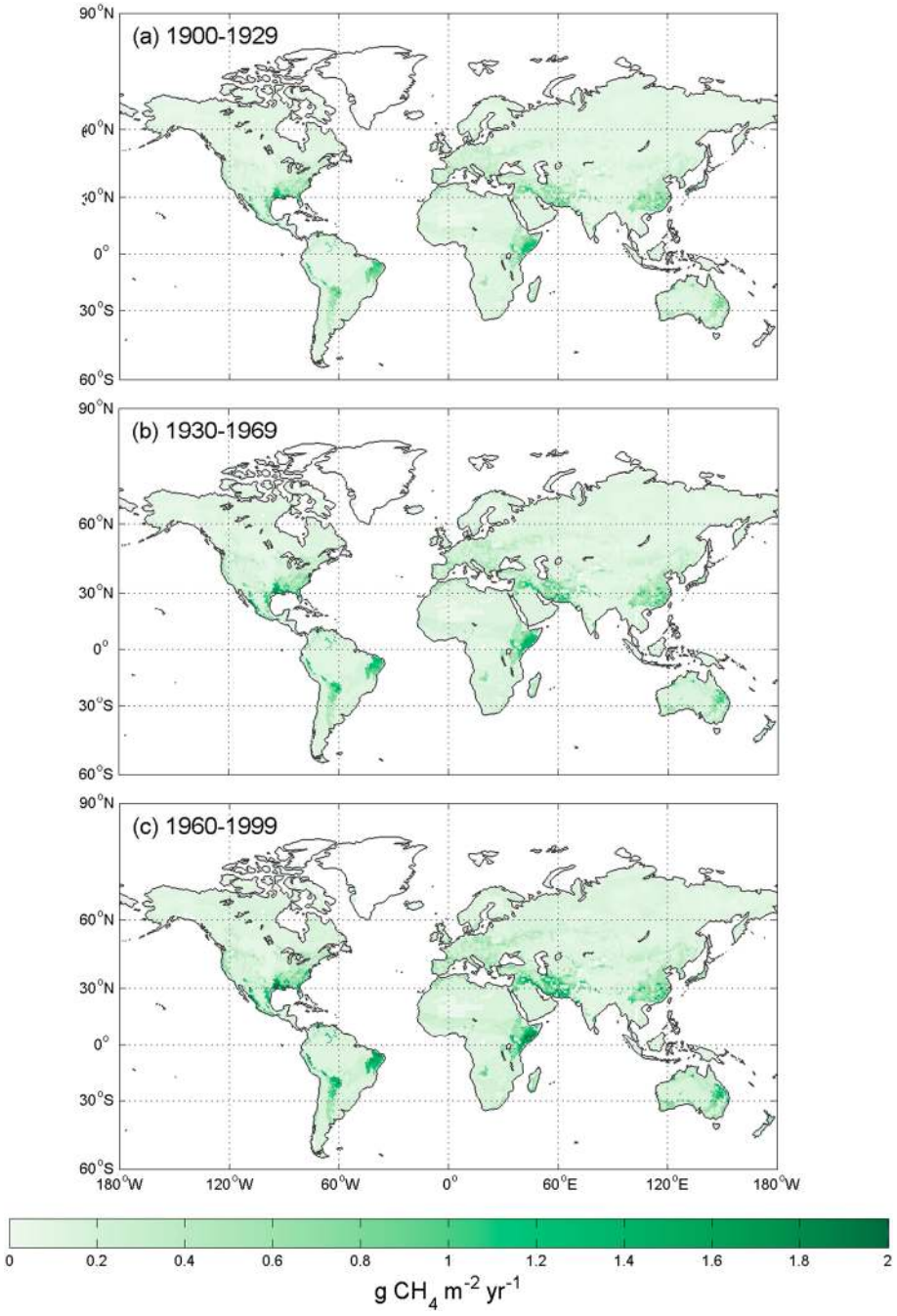

Figure 5. Mean annual global methane consumption (g CH_4 m^{-2} yr^{-1}) for the three periods of (a) 1900–1929, (b) 1930–1969, and (c) 1960–1999. The estimates are derived from the simulation (S4) driven with climate, changes of atmospheric CH_4 concentrations, land use and land cover change, and atmospheric deposition of NH_x with 2 year lag effects.

the human population in year 1993. The scaled data were then interpolated to a 0.5° resolution using the nearest neighborhood method (Figure 2).

[23] To conduct simulations for the 21st century, we utilized climate forcing data sets based on the Intergovernmental Panel on Climate Change (IPCC) future climate scenarios, which represent possible future climates under emissions scenarios from extreme to moderate: (1) more integrated world with rapid economic growth with an emphasis on fossil fuels (A1FI); (2) more divided world with regionally oriented economic development (A2); (3) more divided world but more ecologically friendly (B2); and (4) more integrated world and rapid economic growth but ecologically friendly (B1) [*International Panel on Climate Change*, 2000, 2001]. Under those scenarios, the global climate has been simulated with Hadley Centre Coupled Model, version 3 and processed to a 0.5° × 0.5° spatial resolution [*Mitchell et al.*, 2004]. The transient atmospheric CH_4 concentration data were obtained by linearly interpolating the decadal data for these four future scenarios (Figure 3). For N deposition, we assumed

Table 4. Global Soil Methane Consumption in Different Natural and Agricultural Ecosystems in the 1990s

Vegetation Types	Upland Area (Million km^2)	CH_4 Tg CH_4 yr^{-1})
Alpine Tundra	4.70	0.46
Wet Tundra	4.24	0.72
Boreal Forest	8.40	0.93
Forested Boreal Wetlands	1.77	0.02
Boreal Woodlands	5.13	0.79
Non-Forested Boreal Wetlands	0.47	0.05
Mixed Temperate Forests	3.08	2.53
Temperate Coniferous Forests	1.98	1.67
Temperate Deciduous Forests	2.05	1.23
Temperate Forested Wetlands	0.03	0.04
Tall Grasslands	1.67	0.22
Short Grasslands	3.42	0.59
Tropical Savannas	9.57	1.87
Xeric Shrublands	12.95	1.75
Tropical Evergreen Forests	12.31	0.05
Tropical Forested Wetlands	0.32	0.03
Tropical Deciduous Forests	2.68	0.04
Xeric Woodlands	4.69	5.59
Tropical Forested Floodplains	0.05	0.01
Deserts	11.24	1.50
Tropical Non-Forested Wetlands	0.01	0.00
Tropical Non-Forested Floodplains	0.09	0.01
Temperate Non-Forested Wetlands	0.12	0.01
Temperate Forested Floodplains	0.03	0.02
Temperate Non-Forested Floodplains	0.02	0.00
Wet Savannas	0.07	0.00
Salt Marsh	0.05	0.00
Mangroves	0.06	0.00
Tidal Freshwater Marshes	0.00	0.00
Temperate Savannas	4.06	3.01
Agricultural Ecosystems	15.02	5.13
Temperate Evergreen Broadleaf	2.36	2.45
Mediterranean Shrublands	1.10	0.95
Total	113.74	31.67

the annual deposition holds at the year 2000 level for the period 2000–2049 and the year 2050 level for the period 2050–2100 due to the limited availability of global spatially explicit atmospheric N deposition data provided by *Dentener* [2006]. Spatial data of vegetation, soil texture, soil pH, and upland and cropland distributions used in the 21st century were the same data as in the 20th century simulations.

2.5. Simulation Design

[24] For the twentieth century, we conducted four "core" simulations with the set of parameters for both natural and agricultural ecosystems at the global scale: (1) the first simulation was done with an atmospheric CH_4 concentration of year 2000 at 0.075 μM (1700 ppb), but driven with transient climate throughout the century (hereafter referred to as S1); (2) the second simulation was driven with transient climate and atmospheric CH_4 concentrations (hereafter referred to as S2); (3) the third simulation was driven with transient climate, atmospheric CH_4 concentrations, and NH_x deposition (hereafter referred to as S3); and (4) the fourth simulation was driven with transient data of climate, CH_4 concentrations, NH_x deposition, and land use and land cover change (hereafter referred to as S4). To examine the sensitivity of the global consumption to climate, atmospheric CH_4 concentrations, and N deposition, we conducted another eight simulations with the set of parameters by altering air temperature uniformly with ±3°C for each grid cell, precipitation by ±15%, atmospheric CH_4 concentrations by ±35% changes, and NH_x deposition by ±25%, respectively, while maintaining all other variables to be the same as in the original data. In these simulations, NH_x deposition was assumed to have a 2 year lag inhibitive effect on methanotrophy according to field studies [e.g., *Schnell and King*, 1994]. To further constrain the estimates, we conducted another simulation driven with the climate data from the European Centre for Medium-Range Weather Forecasts (ECMWF) from 1998 to 2008 (http://data-portal.ecmwf.int/data/d/interim_daily/), but otherwise with the same forcing as in the S4 simulation with 2 year NH_x lag effects (hereafter referred to as S4b simulation).

[25] For the 21st century, we conducted two sets of simulations under the above four IPCC climate scenarios. The first set of simulations assumes that the global NH_x deposition remains at the level of year 2000 throughout the century. The second set of simulations is driven with the N deposition data as described above.

3. Results

3.1. Global Soil Methane Consumption During the Twentieth Century

[26] During the twentieth century, the soil methane consumption increase rate was 0.14 Tg CH_4 yr^{-2}, from 18 Tg CH_4 yr^{-1} in the first decade to 32 Tg CH_4 yr^{-1} in the 1990s under changing conditions of climate, atmospheric CH_4 concentrations, land use change, and N deposition (Figure 4). Natural ecosystems dominated the consumption, while agricultural ecosystems were only responsible for 16% of the total global soil consumption (Table 3). The average maximum consumption was 3.24 Tg CH_4 month^{-1} in July, and the average minimum consumption was 1.30 Tg CH_4 month^{-1} in February during the century. Seasonal amplitude increased from 1.44 in the 1900s to 3.13 Tg CH_4 month^{-1} during the 1990s.

[27] At the global scale, the consumption increased from north to south (Figure 5). This north-south gradient prevails throughout the twentieth century. This simulated north-south gradient may be biased due to the limited number of parameterization sites in the south (Table 1). With time, there was no significant change in the consumption in the Northern Hemisphere, but a significant enhancement of the consumption occurred in the Southern Hemisphere. The region between 45°S and 45°N was responsible for more than 80% of the total global consumption (Table 3). The southern United States, eastern China, South America, and Australia had relatively high consumption rates (Figure 5). As a result, the northern high latitudes (45°N–90°N) consumed about 5 Tg CH_4 yr^{-1}. The United States, China, and Australia consumed 2.84, 2.78, and 2.89 Tg CH_4 yr^{-1}, respectively, during the 1990s. The Sahara desert also had a large consumption of 1.36 Tg CH_4 yr^{-1}.

[28] The global soil consumption varied with ecosystem types with more than 80% of the consumption in natural ecosystem soils (Table 4). The agricultural ecosystems soils only consumed about 5.13 Tg CH_4 yr^{-1}. Tundra ecosystems and boreal forests, occupying 8.8 million km^2, took up 1.18 and 1.79 Tg CH_4 yr^{-1}, respectively. Temperate forests and grasslands were moderate sinks

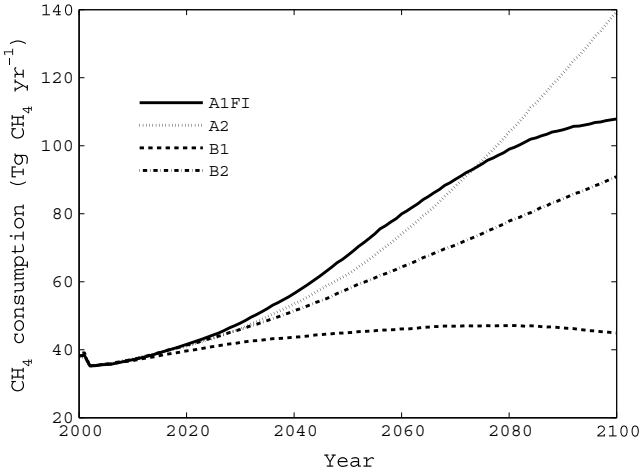

Figure 6. Future global soil methane consumption under different climate scenarios simulated with a 2 year NH_x effect.

and were responsible for 5.47 and 0.81 Tg CH_4 yr^{-1}, respectively. In contrast, xeric woodlands and shrublands accounted for more than 25% of the total global soil consumption. Deserts consumed 1.50 Tg CH_4 yr^{-1} over their 11 million km^2 area. Temperate savannas with an area of 4 million km^2 also acted as a significant sink of 3.01 Tg CH_4 yr^{-1}. However, tropical evergreen forests occupied a large land area of 12 million km^2, but only consumed 0.05 Tg CH_4 yr^{-1}. Overall, the annual soil methane consumption was higher in areas with sparser vegetation, ranking downward from deserts to shrublands, to grasslands, and then finally to forest ecosystems.

[29] The S1, S2, and S3 simulations estimated global total consumption rates ranging from 32 to 36 Tg CH_4 yr^{-1} in the 1990s (Table 3). The S1 simulation, driven with a constant atmospheric CH_4 level and transient climate, showed a steady soil methane consumption rate of 36 Tg CH_4 yr^{-1} during the twentieth century, while the S2, S3, and S4 simulations showed an increasing trend (Figure 4). In S4b simulation driven with ECMWF data, we estimated the global consumption is 33 Tg CH_4 yr^{-1} during the period 1989–2008.

3.2. Global Soil Methane Consumption During the 21st Century

[30] Under future climate conditions, atmospheric CH_4 concentrations and N deposition scenarios, global soil consumption is predicted to increase with rates ranging from 0.05 to 1.0 Tg CH_4 yr^{-2} during the 21st century (Figure 6). Holding the N deposition at the level of the year 2000, our simulations of global soil methane consumption range from 45 to 140 Tg CH_4 yr^{-1} by the end of the century. The second set of future simulations with different levels of N deposition before 2050 and after 2050 estimate that the global total only decreases 1% in comparison with the first set of future simulations at the end of the 21st century.

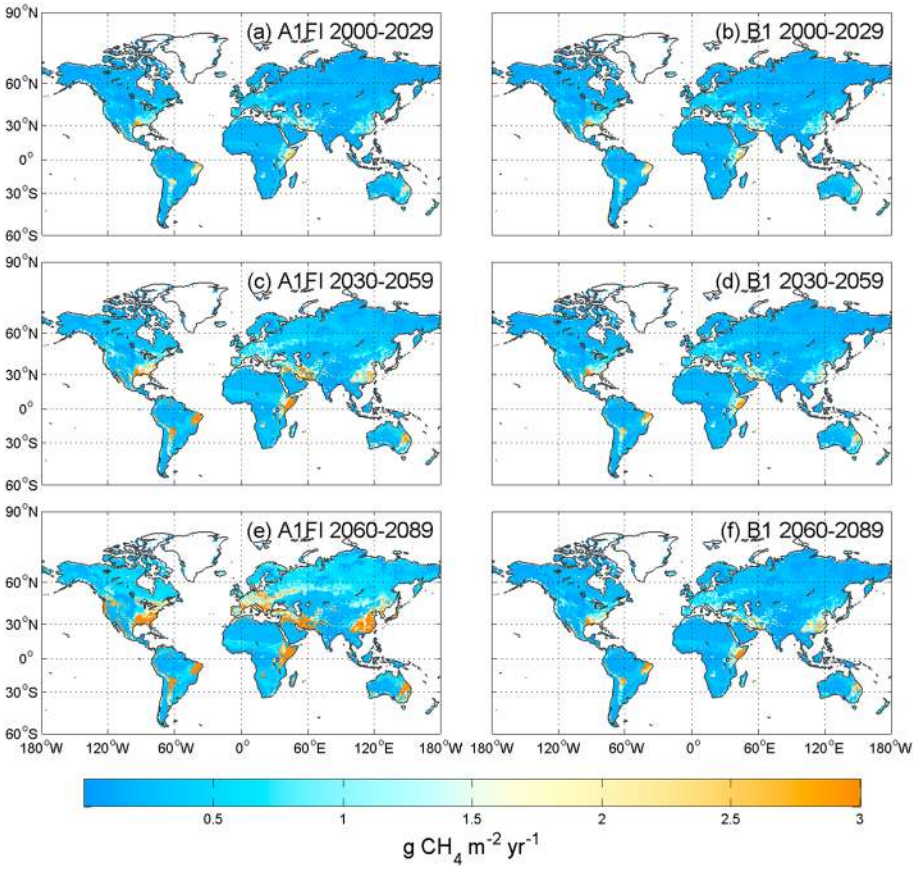

Figure 7. Global methane consumption under future climate scenarios (A1FI and B1) partitioned to every 30 year period. The values are mean annual consumption of the 30 year average.

Table 5. Effects of Climate, Annual Soil Temperature at Top 20 cm Depth, and Soil Moisture on Consumption for Different Regions and the Globe During the Twentieth Century[a]

	Annual Air Temperature	Annual Precipitation	Methane Mixing Ratio	NH_x Deposition	Soil Temperature	Soil Moisture
45°S South	0.17	−0.12	0.99[b]	0.92[b]	0.18	0.98[b]
0°S–45°S	0.68[b]	0.37[b]	1.00[b]	0.94[b]	0.68[b]	1.00[b]
0°N–45°N	0.69[b]	0.06	0.99[b]	0.93[b]	0.68[b]	1.00[b]
45°N North	0.63[b]	0.74[b]	0.98[b]	0.83[b]	0.68[b]	0.99[b]
Global	0.69[b]	0.57[b]	0.99[b]	0.92[b]	0.74[b]	1.00[b]

[a]The simulated consumption is based on transient atmospheric methane concentrations, changes of NH_x deposition, and transient climate with 2 year NH_x year lag effects. The values are Pearson correlations between annual methane consumption and environmental factors.
[b]$p < 0.01$.

[31] Spatial patterns of the consumption varied in different future scenarios as a result of changes in climate and atmospheric CH_4 concentrations, as well as N deposition rates (Figure 7). Specifically, under the scenarios A1FI, A2, and B2, the sink in the eastern and western U.S. and the eastern China was strengthened. South America and Australia became even stronger sink regions compared to their current sinks. The increasing consumption rate in boreal regions led to a larger global total sink. In contrast, similar sink rates to the current sink levels remained in scenario B1 at the end of the 21st century.

[32] By the end of the 21st century, under the scenarios A1FI, A2, B1, and B2, boreal ecosystems consumed up to 5–20 Tg CH_4 yr^{-1}. In contrast, tropical ecosystems retained similar sink strengths in 2100 in comparison to the present. Shrubland and woodland ecosystems became even stronger sinks ranging in 2100 from 12 to 38 Tg CH_4 yr^{-1}. Throughout the century, tundra and grassland ecosystems remained as moderate sinks, of 2–13 Tg CH_4 yr^{-1}, respectively. As a result, the United States and China each consumed in 2100 about 5–20 Tg CH_4 yr^{-1}, and Australia consumed 3–11 Tg CH_4 yr^{-1} with its sink area becoming even larger. Similarly, Russia and Canada increased their sinks by 2100 to 3–11 and 2–8 Tg CH_4 yr^{-1}, respectively.

4. Discussion

4.1. Comparison With Other Studies

[33] For the 1990s, our estimates of global soil consumption of 32–36 Tg CH_4 yr^{-1} are significantly constrained in comparison with the range of 17–51 Tg CH_4 yr^{-1} obtained from other existing estimates using various process-based and bookkeeping modeling approaches [e.g., *Ridgwell et al*., 1999; *Curry*, 2007; *King*, 1997; *Potter et al*., 1996; *Dutaur and Verchot*, 2007; *Dorr et al*., 1993; *Smith et al*., 2000]. The differences among models are due to several factors being considered differently in various studies as enumerated by *King* [1997]. For instance, *Curry* [2007] estimates that considering the effects of temperature, moisture, and land cultivation, the global sink strength is between 9 and 47 with an average of 28 Tg CH_4 yr^{-1}. His analysis suggests that the sensitivity of consumption is more severe to soil moisture than to air temperature. In his study, deserts are not factored into the calculations. We estimated that deserts, however, while accounting for 10% of the global land area, consume only 1.50 Tg CH_4 yr^{-1} (Table 4). This estimate is lower than an estimate based on an observed consumption rate of 0.66 mg CH_4 m^{-2} d^{-1} of a desert in the U.S. [*Striegl et al*., 1992]. Spatially, our simulations also estimated that warmer and drier soils in semiarid steppe, tropical savanna, tropical seasonal forest, and chaparral ecosystems consume the most methane [e.g., *Potter et al*., 1996]. This is primarily due to a higher atmospheric CH_4 diffusion rate into soils in these ecosystems, while climatology and soil wetness conditions and NHx deposition also contribute to the spatial variability. Our parameterization sites are more in midlatitudes of the Northern Hemisphere and less in tropical regions and the Southern Hemisphere, which may also contribute to the spatial simulation results (Table 1). *Smith et al*. [2000] found that in situ data of methane oxidation follow lognormal distributions. Ideally, we could parameterize the model based on the distribution of the observed data to quantify the regional consumption uncertainty. However, due to lack of time series data, we were not able to do such quantification.

[34] For the future, we estimated that the global soil consumption increases 22% to 280% depending on what IPCC Special Report on Emissions Scenarios (SRES) (A1FI, A2, B1, and B2) are used. Due mainly to a relatively larger temperature response, the northern high latitudes had relatively more enhanced consumption rates in comparison to the Southern Hemisphere (Figure 7). *Curry* [2009] also finds that under the SRES emission scenario A1B, the model projects a 23% increase in the global annual mean CH_4 soil consumption by 2100, and the largest relative increases occur in the northern high latitudes.

Table 6. Sensitivity Studies of Global Soil Methane Consumption to Changes in NH_x Lag Effects, Atmospheric Methane Concentration, NH_x Deposition, Air Temperature (AT), and Precipitation[a]

	Baseline	NH_x 10 Years	CH_4 +30%	CH_4 −30%	NH_x +25%	NH_x −25%	Precipitation +15%	Precipitation −15%	AT +3° C	AT −3° C
Consumption (Tg CH_4 yr^{-1})	31.7	27.6	40.5	23.6	29.0	32.7	32.0	32.0	41.7	25.0
Changes (%)	0.0	−13	28	−25	−9	3	0.9	0.9	32	−21

[a]The values are for the 1990s. The simulations are conducted using transient climate with baseline as well as the following nine sensitivity runs: (1) 10 year lag in NH_x; (2) 30% increase in atmospheric CH_4; (3) 30% decrease in atmospheric CH_4; (4) 25% increase in NH_x; (5) 25% decrease in NH_x; (6) 15% increase in precipitation; (7) 15% decrease in precipitation; (8) 3°C increase in air temperature; and (9) 3°C decrease in air temperature. Percentage changes are calculated based on these S4 sensitivity simulations.

Table 7. Role of Global Soil Methane Consumption in Atmospheric CH_4 Mole Fraction During the Period of 1998–2004[a]

	S1	S2	S3
RMSD of atmospheric CH_4 mole fraction (ppb $month^{-1}$)	3.9	4.4	0.2
Difference of atmospheric CH_4 mole fraction in December of 2004 (ppb)	6.2	7.1	0.5
RMSD of global monthly soil consumption (Tg CH_4 $month^{-1}$)	0.3	0.4	0.1
Difference of cumulative global soil methane consumption in the end of 2004 (Tg CH_4 $period^{-1}$)	24.5	27.6	1.8

[a]Differences and root-mean-square differences (RMSD) are calculated with S4 simulation as a baseline. Monthly atmospheric CH_4 mole fractions are calculated with the atmospheric transport chemistry model MOZART.

4.2. Major Controls to Soil Methane Consumption

[35] During the twentieth century, the consumption increase rate was primarily due to increasing soil temperature resulted from increasing air temperature, moisture, nitrogen deposition, and atmospheric methane concentrations (Table 5). This temperature response is consistent with our sensitivity analysis for the 1990s, which indicates that a 3°C air temperature increase will result in a 21–32% change in global soil methane consumption (Table 6). Our simulations under future climate scenarios also indicated that the increasing surface temperature dominates the future sink strength (Figures 3 and 6). In contrast, *Ridgwell et al*. [1999] assumed less sensitive temperature response of methane oxidation activity in high temperatures (i.e., >20°C), suggesting that global warming will leave the global methane sink unchanged, and concluded that the microbial activity is instead the major control.

[36] Soil moisture significantly correlates with consumption, due to moisture effects on physical limitations of atmospheric CH_4 diffusion into soils and microbial activities ($R > 0.98$) (Table 5). However, there is a smaller and even a negative correlation between precipitation and consumption at the global scale and in the south of 45°S. This is consistent with field studies suggesting that higher precipitation reduced CH_4 uptake when either temperature or N deposition (but not both) is increased [*Blankinship et al*., 2010]. *Ridgwell et al*. [1999] concluded that the role of soil moisture in limiting uptake due to inhibition of diffusion is not a major factor. Indeed, in our study, a 15% change in annual precipitation did not affect consumption significantly. We found that soil moisture has not been changed to a significant level from the 15% precipitation change in our simulations, and consequently, both the amount of atmospheric methane diffusion to soils and the consumption from affected microbial activity have not been impacted significantly.

[37] Decreasing or increasing atmospheric methane concentrations by 30% resulted in a $-25 \sim 28\%$ change in consumption (Table 6). During the twentieth century, rising atmospheric CH_4 concentrations increased the soil consumption by 46% (Figure 4). In contrast, the increasing nitrogen deposition rate suppressed soil CH_4 consumption (Table 6). Since the inhibition from a single application of ammonium can persist for days to months, even after the added ammonium is no longer detectable [*Nesbit and Breitenbeck*, 1992; *Mosier et al*., 1991], we conducted a simulation considering a10 year nitrogen lag effect, which indicated that consumption is reduced by 10% in comparison with simulations run under 2 year lag effect. With the model sensitivity, our simulations S3 and S2 suggested that nitrogen deposition change reduces the global consumption by 10% in the 1990s (Table 3).

[38] Our simulations estimated that 15 Mkm^2 agricultural soils consume 5.13 Tg CH_4 yr^{-1} in the 1990s (Table 3). We have not modeled how land use change due to forest conversion, agricultural abandonment, and urbanization affects the soil consumption. *Menyailo et al*. [2008] showed that afforestation on a well-aerated grassland in Siberia reduces soil CH_4 uptake by a factor of 3 after 35 years of tree growth. The decline in CH_4 oxidation was due to the reduction in biomass in soils and to a lesser extent by reduced cell-specific activity of CH_4 oxidizing bacteria when grasslands were converted to forests. These effects of land use and land cover change should be factored into our future consumption analysis.

4.3. Implication of Global Soil Consumption to Atmospheric Methane Burden

[39] To assess the role of soil uptake in estimating atmospheric methane mixing ratios, we ran MOZART v4 [*Emmons et al*., 2010] using our four simulation results (S1, S2, S3, and S4). The horizontal resolution of the model is 1.9° latitude × 2.5° longitude with 56 vertical levels from the surface up to approximately 2 mb. The chemical and transport processes in the model are driven by the meteorological fields from the Modern Era Retrospective-analysis for Research and Applications (MERRA), which have interannual variability [*Rienecker et al*., 2011].

[40] For emissions other than methane consumption (for which we used the simulated values from TEM), we used the Goddard Institute for Space Studies (GISS) data set (for details, see *Fung et al*. [1991]). The GISS data set includes emissions from animals, landfills, venting of natural gas at wells, pipeline leakage of natural gas, coal mining, termites, hydrates/clathrates, rice cultivation, wetland ecosystems, forested and non-forested bogs, forested and non-forested swamps and alluvial formation, tundra, and biomass burning. In our simulations, these sink and source data were updated with more recent annually-varying emissions including the Advanced Global Atmospheric Gases Experiment (AGAGE v4.2) for anthropogenic sources (http://agage.eas.gatech.edu/data.html) [*Prinn et al*., 2000], Global Fire Emissions Database version 3.1 for biomass burning [*Van der Werf et al*., 2010], and Community Land Model version 4 for wetlands emissions [*Melton et al*., 2012].

[41] We assumed that the loss mechanism for atmospheric CH_4 only included the reaction with hydroxyl radical (OH) and O^1D, and these fields were taken from *Patra et al*. [2011]. We scaled the spatial and temporal pattern of the annually repeating (i.e., no long-term trend) OH field using measurements of methyl chloroform (CH_3CCl_3) and a three-dimensional climatological OH distribution [*Spivakovsky et al*., 2000], applying a methodology as analyzed earlier [*Prinn et al*., 2005]. The lifetime of CH_4 using these chemical fields and the emissions data mentioned above was approximately 10 years, which is similar to other current estimates

of its lifetime [*Boucher et al*., 2009]. We ran the model with an initial condition constructed with a latitudinal as well as a vertical gradient and did a spin-up using constant emissions and interannual meteorology from 1990 to the end of 1998. We then ran our four simulations from 1998 until the end of 2004.

[42] Since other sinks and sources and transport are kept the same, but the soil consumption rates are allowed to change in our simulations, the comparisons between the simulation S4 and the other simulations allowed us to assess the relative role of soil methane consumption in affecting atmospheric CH_4 ratios. During 1998–2004, the largest root-mean-square differences (RMSD) of global soil consumption were 0.40 Tg CH_4 $month^{-1}$ between S2 and S4 simulations, resulting in 28 Tg CH_4 more methane in the atmosphere by the end of 2004. This consumption difference causes 7.1 ppb higher methane mixing ratios in the atmosphere in December of 2004 (Table 7). Comparing the S3 with S4 simulations, we found that the global soil methane consumption induced by agricultural soils played a minor role in affecting atmospheric CH_4 mole fractions. In contrast, comparing the S2 and S3 simulations, N deposition suppressed the total methane sink by 26 Tg during the period; as a result, the atmospheric CH_4 mole fraction of the S3 simulation was 6.6 ppb higher than the estimates based on the S2 simulation in December of 2004. During this period, a cumulative increase of every 1 Tg of soil CH_4 consumption will decrease atmospheric CH_4 mole fractions about 0.26 ppb. The large uncertainty in global soil CH_4 consumption due to limited knowledge about the effects of climate, atmospheric nitrogen deposition, and land use will result in diverse atmospheric CH_4 mole fraction estimates.

5. Conclusions

[43] The effects of multiple factors on the global atmospheric CH_4 soil consumption rate were analyzed for the 20th and 21st centuries using a process-based biogeochemistry model. The processes associated with the factors including nitrogen deposition, rising atmospheric CH_4 concentrations, agricultural land use, and changing climate are modeled. We found that agricultural land and N deposition changes play minor and moderate roles in determining soil methane consumption, respectively. We estimated that global soils consumed 32–36 Tg CH_4 yr^{-1} during the 1990s and that natural ecosystems are the major sinks while agricultural ecosystems only consume 5.13 Tg CH_4 yr^{-1}. During the twentieth century, the consumption rates and seasonal amplitudes (the differences between the lowest and highest monthly consumption during a year) increased mainly due to a warming climate. Arid areas like deserts, shrublands, and xeric woodlands were sink hot spots for consumption. During the 21st century, the projected global soil consumption persistently increased under different future climate scenarios. While dry areas persisted as sinks in the projections, boreal ecosystems became stronger sinks mainly due to increasing soil temperatures. Nitrogen deposition would modestly reduce the future sink strength at the global scale. Our global atmospheric chemical transport model simulations indicated that the global soil methane consumption reduced by nitrogen deposition increased the atmospheric CH_4 ratios by 6.6 ppb during the period 1998–2004. On average, a cumulative increase of every 1 Tg soil CH_4 consumption will change atmospheric CH_4 mole fractions by about 0.26 ppb during the period 1998–2004. More accurate quantification of soil sink therefore deserves attention for future Earth system modeling.

[44] **Acknowledgments.** This research is supported by the National Aeronautics and Space Administration (NASA) Land Use and Land Cover Change program (NASA-NNX09AI26G), Department of Energy (DE-SC0007007, DE-FG02-06ER64320 and DE-FG02-94ER61937 to MIT), National Science Foundation (NSF-1028291 and NSF-0919331), the NSF Division of Information and Intelligent Systems (NSF-1028291), and the NSF Carbon and Water in the Earth program (NSF-0630319). The computing is supported by Rosen Center of high-performance computing at Purdue. This study is a contribution to a Working Group of "Toward an adequate quantification of CH_4 emissions from land ecosystems: Integrating field and in-situ observations, satellite data, and modeling," supported by the National Center for Ecological Analysis and Synthesis, a center funded by NSF (grant DEB-0553768), the University of California, Santa Barbara, and the State of California.

References

Bergamaschi, P., M. Krol, F. Dentener, A. Vermeulen, F. Meinhardt, R. Graul, M. Ramonet, W. Peters, and E. J. Dlugokencky (2005), Inverse modelling of national and European CH_4 emissions using the atmospheric zoom model TM5, *Atmos. Chem. Phys.*, *5*, 2431–2460.

Bergamaschi, P., et al. (2009), Inverse modeling of global and regional CH_4 emissions using SCIAMACHY satellite retrievals, *J. Geophys. Res.*, *114*, D22301, doi:10.1029/2009JD012287.

Blankinship, J. C., J. R. Brown, P. Dijkstra, and B. A. Hungate (2010), Effects of interactive global changes on methane uptake in an annual grassland, *J. Geophys. Res.*, *115*, G02008, doi:10.1029/2009JG001097.

Born, M., H. Dörr, and I. Levin (1990), Methane consumption in aerated soils of the temperate zone, *Tellus, Ser. B.*, *42*, 2–8.

Boucher, O., P. Friedlingstein, B. Collins, and K. P. Shine (2009), The indirect global warming potential and global temperature change potential due to methane oxidation, *Environ. Res. Lett.*, *4*, 044007, doi:10.1088/1748-9326/4/4/044007.

Bousquet, P., D. A. Hauglustaine, P. Peylin, C. Carouge, and P. Ciais (2005), Two decades of OH variability as inferred by an inversion of atmospheric transport and chemistry of methyl chloroform, *Atmos. Chem. Phys.*, *5*, 2635–2656, doi:10.5194/acp-5-2635-2005.

Bousquet, P., et al. (2006) Contribution of anthropogenic and natural sources to atmospheric methane variability, *Nature*, *443*, 439–443, doi:10.1038/nature05132.

Butler, T. M., I. Simmonds, and P. J. Rayner (2004), Mass balance inverse modelling of methane in the 1990s using a chemistry transport model, *Atmos. Chem. Phys.*, *4*, 2561–2580.

Cao, M., J. B. Dent, and O. W. Heal (1995), Modeling methane emissions from rice paddies, *Global Biogeochem. Cyles*, *9*, 183–195.

Carter, A. J., and R. J. Scholes (2000), Soil data v2.0: Generating a global database of soil properties, report, Counc. for Sci. and Ind. Res., Pertoria, South Africa.

Castro, M. S., P. A. Steudler, J. M. Melillo, J. D. Aber, and R. D. Bowden (1995), Factors controlling atmospheric methane consumption by temperate forest soils, *Global Biogeochem. Cycles*, *9*(1), 1–10, doi:10.1029/94GB02651.

Chan, A. S. K., and T. B. Parkin (2001), Effect of land use on methane flux from soil, *J. Environ. Qual.*, *30*(3), 786–797.

Chen, Y.-H., and R. G. Prinn (2006), Estimation of atmospheric methane emissions between 1996 and 2001 using a three-dimensional global chemical transport model, *J. Geophys. Res.*, *111*, D10307, doi:10.1029/2005JD006058.

Cunnold, D. M., et al. (2003), In situ measurements of atmospheric methane at GAGE/AGAGE sites during 1985–2000 and resulting source inferences, *J. Geophys. Res.*, *107*(D14), 4225, doi:10.1029/2001JD001226.

Curry, C. L. (2007), Modeling the soil consumption of atmospheric methane at the global scale, *Global Biogeochem. Cyles*, *21*, GB4012, doi:10.1029/2006GB002818.

Curry, C. (2009), The consumption of atmospheric methane by soil in a simulated future climate, *Biogeosciences*, *6*, 2355–2367.

Dentener, F. J. (2006), Global maps of atmospheric nitrogen deposition, 1860, 1993, and 2050, http://daac.ornl.gov/, Oak Ridge Natl. Lab. Distrib. Active Arch. Cent., Oak Ridge, Tenn.

Dentener, F., W. Peters, M. Krol, M. van Weele, P. Bergamaschi, and J. Lelieveld (2003), Interannual variability and trend of CH4 lifetime as a measure for OH changes in the 1979–1993 time period, *J. Geophys. Res.*, *108*(D15), 4442, doi:10.1029/2002JD002916.

Dlugokencky, E. J., E. G. Dutton, P. C. Novelli, P. P. Tans, K. A. Masarie, K. O. Lantz, and S. Madronich (1996), Changes in CH_4 and CO growth

rates after the eruption of Mt Pinatubo and their link with changes in tropical tropospheric UV flux, *Geophys. Res. Lett.*, *23*, 2761–2764.

Dlugokencky, E. J., S. Houweling, L. Bruhwiler, K. A. Masarie, P. M. Lang, J. B. Miller, and P. P. Trans (2003), Atmospheric methane levels off: Temporary pause or a new steady state? *Geophys. Res. Lett.*, *30*(19), 1992, doi:10.1029/ 2003GL018126.

Dlugokencky, E. J., R. C. Myers, P. M. Lang, K. A. Masarie, A. M. Crotwell, K. W. Thoning, B. D. Hall, J. W. Elkins, and L. P. Steele (2005), Conversion of NOAA atmospheric dry air CH_4 mole fractions to a gravimetrically prepared standard scale, *J. Geophys. Res.*, *110*, D18306, doi:10.1029/2005JD006035.

Dlugokencky, E. J., et al. (2009), Observational constraints on recent increases in the atmospheric CH_4 burden, *Geophys. Res. Lett.*, *36*, L18803, doi:10.1029/2009GL039780.

Dobbie, K. E., and K. A. Smith (1996), Comparison of CH_4 oxidation rates in woodland, arable and set aside soils, *Soil Biol. Biochem.*, *28*(10–11), 1357–1365.

Dorr, H., L. Katru, and I. Levin (1993), Soil texture parameterization of the methane uptake in aerated soils, *Chemosphere*, *26*, 697–713.

Dutaur, L., and V. Verchot (2007), A global inventory of the soil CH_4 sink, *Global Biogeochem. Cyles*, *21*, GB4013, doi:10.1029/ 2006GB002734

Emmons, L. K., et al. (2010), Description and evaluation of the Model for Ozone and Related chemical Tracers, version 4 (MOZART-4), *Geosci. Model Dev.*, *3*, 43–67.

Etheridge, D. M., L. P. Steele, R. J. Francey, and R. L. Langenfields (1998), Atmospheric methane between 1000 A.D. and present: Evidence of anthropogenic emissions and climatic variability, *J. Geophys. Res.*, *103*, 15,979–15,993.

Flessa, H., P. Dörsch, and F. Beese (1995), Seasonal variation of N_2O and CH_4 fluxes in differently managed arable soils in southern Germany, *J. Geophys. Res.*, *100*, 23,115–23,124, doi:10.1029/95JD02270.

Forster, P., et al. (2007), Changes in atmospheric constituents and in radiative forcing, in *Climate Change 2007: The Physical Science Basis. Contribution of Working Group I to the Fourth Assessment Report of the Intergovernmental Panel on Climate Change*, 996 pp., edited by S. Solomon et al., Cambridge Univ. Press, Cambridge, U.K.

Frankenberg, C., P. Bergamaschi, A. Butz, S. Houweling, J. F. Meirink, J. Notholt, A. K. Petersen, H. Schrijver, T. Warneke, and I. Aben (2008), Tropical methane emissions: A revised view from SCIAMACHY onboard Envisat, *Geophys. Res. Lett.*, *35*, L15811, doi:10.1029/2008GL034300.

Fung, I., J. John, J. Lerner, E. Matthews, M. Prather, L. P. Steele, and P. J. Fraser (1991), Three-dimensional model synthesis of the global methane cycle, *J. Geophys. Res.*, *96*, 13,033–13,065.

Galloway, J. N., J. D. Aber, J. W. Erisman, S. P. Seitzinger, R. H. Howarth, E. B. Cowling, and B. J. Cosby (2003), The nitrogen cascade, *Bioscience*, *53*, 341–356.

Globalview-CH_4 (2005), Cooperative Atmospheric Data Integration Project —Methane [CD-ROM], Global Monit. Div., Earth Syst. Res. Lab., NOAA, Boulder, Colo, [Available at ftp.cmdl.noaa.gov/ccg/ch4/ GLOBALVIEW].

Hein, R., P. J. Crutzen, and M. Heimann (1997), An inverse modeling approach to investigate the global atmospheric methane cycle, *Global Biogeochem. Cycles*, *11*, 43–76.

Houweling, S., T. Kaminski, F. Dentener, J. Lelieveld, and M. Heimann (1999), Inverse modeling of methane sources and sinks using the adjoint of a global transport model, *J. Atmos. Res.*, *104*(D21), 26,137–26,160.

International Panel on Climate Change (2000), *Special Report on Emissions Scenarios: A Special Report of Working Group III of the Intergovernmental Panel on Climate Change*, Cambridge Univ. Press, New York.

International Panel on Climate Change (2001), *Climate Change 2001: IPCC Third Assessment Report*, Cambridge Univ. Press, New York.

Keller, M., W. A. Kaplan, and S. C. Wofsy (1986), Emissions Of N_2O, CH_4 and CO_2 from tropical forest soils, *J. Geophys. Res.*, *91*, 11,791–11,802, doi:10.1029/JD091iD11p11791.

Keller, M., M. E. Mitre, and R. F. Stallard (1990), Consumption of atmospheric methane in soils of central Panama: Effects of agricultural development, *Global Biogeochem. Cycles*, *4*, 21–27, doi:10.1029/ GB004i001p00021.

King, G. M. (1997), Responses of atmospheric methane consumption by soils to global climate change, *Global Change Biol.*, *3*, 351–362.

Krol, M., and J. Lelieveld (2003), Can the variability in tropospheric OH be deduced from measurements of 1,1,1-trichloroethane (methyl chloroform)?, *J. Geophys. Res.*, *108*(D3), 4125, doi:10.1029/2002JD002423, issn:0148–0227.

Lelieveld, J., P. J. Crutzen, and F. J. Dentener (1998), Changing concentration, lifetime and climate forcing of atmospheric methane, *Tellus, Ser. B*, *50*, 128–150.

Matthews, E., and I. Fung (1987), Methane emissions from natural wetlands: Global distribution, area and environmental characteristics of sources, *Global Biogeochem. Cycles*, *1*, 61–86.

McGuire, A. D., et al. (2001), Carbon balance of the terrestrial biosphere in the twentieth century: Analyses of CO_2, climate and land-use effects with four process-based ecosystem models, *Global Biogeochem. Cycles*, *15*, 183–206.

Melillo, J. M., A. D. McGuire, D. W. Kicklighter, B. Moore, III, C. J. Vorosmarty, and A. L. Schloss (1993), Global climate change and terrestrial net primary production, *Nature*, *363*, 234–240.

Melton, J. R., et al. (2012), Present state of global wetland extent and wetland methane modelling: Conclusions from a model intercomparison project (WETCHIMP), *Biogeosci. Discuss.*, *9*, 11577–11654, doi:10.5194/bgd-9-11577-2012.

Menyailo, O. V., B. A. Hungate, W.-R. Abraham, and R. Conrad (2008), Changing land use reduces soil CH_4 uptake by altering biomass and activity but not composition of high-affinity methanotrophs, *Global Change Biol.*, *14*, 2405–2419, doi:10.1111/j.1365-2486.2008.01648.x.

Mikaloff Fletcher, S. E., P. P. Tans, L. M. Bruhwiler, J. B. Miller, and M. Heimann (2004), CH_4 sources estimated from atmospheric observations of CH_4 and its $^{13}C/^{12}C$ isotopic ratios: 1. Inverse modeling of source processes, *Global Biogeochem. Cycles*, *18*, GB4005, doi:10.1029/ 2004GB002224.

Mitchell, T. D., and P. D. Jones (2005), An improved method of constructing a database of monthly climate observations and associated high-resolution grids, *Int. J. Climatol.*, *25*, 693–712, doi:10.1002/joc.1181.

Mitchell, T. D., T. R. Carter, P. D. Jones, M. Hulme, and M. New (2004), A comprehensive set of high-resolution grids of monthly climate for Europe and the globe: The observed record (1901–2000) and 16 scenarios (2001–2100), *Tyndall Working Pap. 55*, Tyndall Cent., Univ. of East Anglia, Norwich, U. K.

Montzka, S. A., M. Krol, E. Dlugokencky, B. Hall, P. Jöckel, and J. Lelieveld (2011), Small interannual variability of global atmospheric hydroxyl, *Science*, *331*, 67–69.

Mosier, A., D. Schimel, D. Valentine, K. Bronson, and W. Parton (1991), Methane and nitrous oxide fluxes in native, fertilized and cultivated grasslands, *Nature 350*, 330–332.

Nesbit, S. P., and G. A. Breitenbeck, (1992), A laboratory study of factors influencing methane uptake by soil, *Agric. Ecosyst. Environ.*, *41*, 39–54.

Patra, P. K., et al. (2011), TransCom model simulations of CH_4 and related species: Linking transport, surface flux and chemical loss with CH_4 variability in the troposphere and lower stratosphere, *Atmos. Chem. Phys.*, *11*, 12,813–12,837, doi:10.5194/acp-11-12813-2011.

Potter, C. S., E. A. Davison, and L. V. Verchot (1996), Estimation of global biogeochemical controls and seasonality in soil methane consumption, *Chemosphere*, *32*, 2219–2246.

Prinn, R. G., et al. (2000), A history of chemically and radiatively important gases in air deduced from ALE/GAGE/AGAGE, *J. Geophys. Res.*, *105*, 17,751–17,792, doi:10.1029/2000JD900141.

Prinn, R. G., et al. (2001), Evidence for substantial variations of atmospheric hydroxyl radicals in the past two decades, *Science*, *292*, 1882–1888.

Prinn, R. G., et al. (2005), Evidence for variability of atmospheric hydroxyl radicals over the past quarter century, *Geophys. Res. Lett.*, *32*, L07809, doi:10.1029/2004GL022228.

Ridgwell, A., S. Marshall, and K. Gregson (1999), Consumption of atmospheric methane by soils: A process-based model, *Global Biogeochem. Cycles*, *13*, 59–70, doi:10.1029/1998GB900004.

Rienecker, M. M., et al. (2011), MERRA: NASA's Modern-Era Retrospective Analysis for Research and Applications, *J. Clim.*, *24*, 3624–3648, doi:10.1175/JCLI-D-11-00015.1.

Rigby, M., et al. (2008), Renewed growth of atmospheric methane, *Geophys. Res. Lett.*, *35*, L22805, doi:10.1029/2008GL036037.

Saxton, K. E., W. J. Rawls, J. S. Romberger, and R. I. Papendick (1986), Estimating generalized soil-water characteristics from texture, *Soil Sci. Soc. Am. J.*, *50*(4), 1031–1036.

Schnell, S., and G. M. King (1994), Mechanistic analysis of ammonium inhibition of atmospheric methane consumption in forest soils, *Appl. Environ. Microbiol.*, *60*(10), 3514–3521.

Segers, R. (1998), Methane production and methane consumption: A review of processes underlying wetland methane fluxes, *Biogeochemistry*, *41*, 23–51.

Singh, S., J. S. Singh, and A. K. Kashyap (1999), Methane consumption by soils of dryland rice agriculture: Influence of varieties and N-fertilization, *Chemosphere*, *38*(1), 175–189.

Smith, T. M., and R. W. Reynolds (2005), A global merged land air and sea surface temperature reconstruction based on historical observations (1880–1997), *J. Clim.*, *18*, 2021–2036.

Smith, K. A., et al. (2000), Oxidation of atmospheric methane in Northern European soils, comparison with other ecosystems, and uncertainties in the global terrestrial sink, *Global Change Biol.*, *6*, 791–803.

Spahni, R., et al. (2011), Constraining global methane emissions and uptake by ecosystems, *Biogeosciences*, *8*, 1643–1665, doi:10.5194/bg-8-1643-2011.

Spivakovsky, C. M., et al. (2000), Three-dimensional climatological distribution of tropospheric OH: Update and evaluation, *J. Geophys. Res.*, *105*, 8931–8980, doi:10.1029/1999JD901006.

Striegl, R. G., T. A. McConnaughey, D. C. Thorstensen, E. P. Weeks, and J. C. Woodward (1992), Consumption of atmospheric methane by desert soils, *Nature*, *357*, 145–147.

Van der Werf, G. R., J. T. Randerson, L. Giglio, G. J. Collatz, M. Mu; P. S. Kasibhatla, D. C. Morton, R. S. DeFries, Y. Jin, and T. T. van Leeuwen (2010), Global fire emissions and the contribution of deforestation, savanna, forest, agricultural, and peat fires (1997–2009), *Atmos. Chem. Phys.*, *10*, 11,707–11,735, doi:10.5194/acp-10-11707-2010.

Walter, B. P., and M. Heimann (2000), A process-based, climate-sensitive model to derive methane emission from natural wetlands: Application to five wetland sites, sensitivity to model parameters, and climate, *Global Biogeochem. Cycles*, *14*, 745–765.

Walter, B. P., M. Heimann, and E. Matthews (2001), Modeling modern methane emissions from natural wetlands, 1. Model description and results, *J. Geophys. Res.*, *106*, 34,189–34,206.

Weier, K. L. (1999), N2O and CH4 emission and CH4 consumption in a sugarcane soil after variation in nitrogen and water application, *Soil Biol. Biochem.*, *31*, 1931–1941.

Zhang, Y., C. Li, C. C. Trettin, H. Li, and G. Sun (2002), An integrated model of soil hydrology, and vegetation for carbon dynamics in wetland ecosystems, *Global Biogeochem. Cycles*, *16*(4), 1061, doi:10.1029/2001GB001838.

Zhang, W., J. Mo, G. Zhou, P. Gundersen, Y. Fang, X. Lu, T. Zhang, and S. Dong (2008), Methane uptake responses to nitrogen deposition in three tropical forests in southern China, *J. Geophys. Res.*, *113*, D11116, doi:10.1029/2007JD009195.

Zhuang, Q., V. E. Romanovsky, and A. D. McGuire (2001), Incorporation of a permafrost model into a large-scale ecosystem model: Evaluation of temporal and spatial scaling issues in simulating soil thermal dynamics, *J. Geophys. Res.*, *106*, 33,649–33,670.

Zhuang, Q., A. D. McGuire, K. P. O'Neill, J. W. Harden, V. E. Romanovsky, and J. Yarie (2002), Modeling the soil thermal and carbon dynamics of a fire chronosequence in Interior Alaska, *J. Geophys. Res.*, *107*(D1), 8147, doi:10.1029/2001JD001244, [Printed *108*(D1), 2003].

Zhuang, Q., A. D. McGuire, J. M. Melillo, J. S. Clein, R. J. Dargaville, D. W. Kicklighter, R. B. Myneni, J. Dong, V. E. Romanovsky, J. Harden, and J. E. Hobbie (2003), Carbon cycling in extratropical terrestrial ecosystems of the Northern Hemisphere during the 20th century: A modeling analysis of the influences of soil thermal dynamics, *Tellus, Ser. B*, *55B*, 751–776.

Zhuang, Q., J. M. Melillo, D. W. Kicklighter, R. G. Prinn, A. D. McGuire, P. A. Steudler, B. S. Felzer, and S. Hu (2004), Methane fluxes between terrestrial ecosystems and the atmosphere at northern high latitudes during the past century: A retrospective analysis with a process-based biogeochemistry model, *Global Biogeochem. Cycles*, *18*, GB3010, doi:10.1029/2004GB002239.

Zhuang, Q. L., J. M. Melillo, M. C. Sarofim, D. W. Kicklighter, A. D. McGuire, B. S. Felzer, A. Sokolov, R. G. Prinn, P. A. Steudler, and S. Hu (2006), CO_2 and CH_4 exchanges between land ecosystems and the atmosphere in northern high latitudes over the 21st century, *Geophys. Res. Lett.*, *33*, L17403, doi:10.1029/2006gl026972.

Zhuang, Q., J. M. Melillo, A. D. McGuire, D. W. Kicklighter, R. G. Prinn, P. A. Steudler, B. S. Felzer, and S. Hu (2007), Net emissions of CH_4 and CO_2 in Alaska: Implications for the region's greenhouse gas budget, *Ecol. Appl.*, *17*(1), 203–212.

Zhuang, Q., J. M. Melack, S. Zimov, K. M. Walter, C. L. Butenhoff, and M. A. K. Khalil (2009), Global methane emissions from wetlands, rice paddies, and lakes, *Eos Trans. AGU*, *90*(5), 37–38.